Optimal length of ZnO nanorods for improving the light-extraction efficiency of blue InGaN light-emitting diodes

Hyun Jeong,[1] Rafael Salas-Montiel,[1] and Mun Seok Jeong[2,3,*]

[1]*Laboratoire de Nanotechnologie et d'Instrumentation Optique, Institut Charles Delaunay, CNRS-UMR 6281, Université de Technologie de Troyes, BP 2060, 10010 Troyes, France*

[2]*Center for Integrated Nanostructure Physics (CINAP), Institute for Basic Science (IBS), Sungkyunkwan University, Suwon 440-746, South Korea*

[3]*Department of Energy Science, Sungkyunkwan University, Suwon 440-746, South Korea*

[*]*mjeong@skku.edu*

Abstract: Optimal length of ZnO nanorods (NRs) on blue InGaN light-emitting diodes (LEDs) was investigated to improve the light-extraction efficiency (LEE) of the LED. X-ray diffraction, photoluminescence spectroscopy, and micro-Raman spectroscopy were employed to determine the structural and optical properties of the ZnO NRs with length of 300 nm and 5 μm grown by a hydrothermal method. From the conventional light output power versus injection current (L-I) measurement, we found that the light output power of the LEDs with 300-nm- and 5-μm-long ZnO NRs was approximately 14.6% and 40.7% greater, respectively, than that of the LED without the ZnO NRs at an operating current of 20 mA. In addition, there were almost no changes to the electrical properties of the ZnO-NR-coated LEDs. The effect of the length of the ZnO NRs on the LEE of the LEDs was theoretically verified with three-dimensional finite-difference time-domain (FDTD) analysis. The FDTD images of the optical power and far-field radiation patterns of the LEDs showed that more photons were guided to the out of the LED by the longer ZnO NRs than by the shorter ZnO NRs grown on the LEDs.

OCIS codes: (130.0250) Optoelectronics; (160.4670) Optical materials; (220.4000) Microstructure fabrication; (230.3670) Light-emitting diodes; (260.2065) Effective medium theory.

References and links

1. H. Morkoç and S. N. Mohammad, "High-luminosity blue and blue-green gallium nitride light-emitting diodes," Science **267**(5194), 51–55 (1995).
2. F. A. Ponce and D. P. Bour, "Nitride-based semiconductors for blue and green light-emitting devices," Nature **386**(6623), 351–359 (1997).
3. J. J. Wierer, A. David, and M. M. Megens, "III-nitride photonic-crystal light-emitting diodes with high extraction efficiency," Nat. Photonics **3**(3), 163–169 (2009).
4. P. Pust, P. J. Schmidt, and W. Schnick, "A revolution in lighting," Nat. Mater. **14**(5), 454–458 (2015).
5. S. Pimputkar, J. S. Speck, S. P. DenBaars, and S. Nakamura, "Prospects for LED lighting," Nat. Photonics **3**(4), 180–182 (2009).
6. J. Kim, H. Woo, K. Joo, S. Tae, J. Park, D. Moon, S. H. Park, J. Jang, Y. Cho, J. Park, H. Yuh, G.-D. Lee, I.-S. Choi, Y. Nanishi, H. N. Han, K. Char, and E. Yoon, "Less strained and more efficient GaN light-emitting diodes with embedded silica hollow nanospheres," Sci. Rep. **3**, 3201 (2013).
7. R.-H. Horng, B.-R. Wu, C.-H. Tien, S.-L. Ou, M.-H. Yang, H.-C. Kuo, and D.-S. Wuu, "Performance of GaN-based light-emitting diodes fabricated using GaN epilayers grown on silicon substrates," Opt. Express **22**(S1 Suppl 1), A179–A187 (2014).
8. Y.-K. Ee, R. A. Arif, N. Tansu, P. Kumnorkaew, and J. F. Gilchrist, "Enhancement of light extraction efficiency of InGaN quantum wells light emitting diodes using SiO2/polystyrene microlens arrays," Appl. Phys. Lett. **91**(22), 221107 (2007).

#246197 Received 16 Jul 2015; revised 22 Aug 2015; accepted 24 Aug 2015; published 25 Aug 2015

9. J. K. Kim, S. Chhajed, M. F. Schubert, E. F. Schubert, A. J. Fischer, M. H. Crawford, J. Cho, H. Kim, and C. Sone, "Light-extraction enhancement of GaInN light-emitting diodes by graded-refractive-index indium tin oxide anti-reflection contact," Adv. Mater. **20**(4), 801–804 (2008).
10. J. K. Kim, T. Gessmann, E. F. Schubert, J.-Q. Xi, H. Luo, J. Cho, C. Sone, and Y. Park, "GaInN light-emitting diode with conductive omnidirectional reflector having a low-refractive-index indium-tin oxide layer," Appl. Phys. Lett. **88**(1), 013501 (2006).
11. T. Fujii, Y. Gao, R. Sharma, E. L. Hu, S. P. DenBaars, and S. Nakamura, "Increase in the extraction efficiency of GaN-based light-emitting diodes via surface roughening," Appl. Phys. Lett. **84**(6), 855–857 (2004).
12. T. K. Kim, S. H. Kim, S. S. Yang, J. K. Son, K. H. Lee, Y. G. Hong, K. H. Shim, J. W. Yang, K. Y. Lim, S. J. Bae, and G. M. Yang, "GaN-based light-emitting diode with textured indium tin oxide transparent layer coated with Al2O3 powder," Appl. Phys. Lett. **94**(16), 161107 (2009).
13. E. Matioli, S. Brinkley, K. M. Kelchner, Y.-L. Hu, S. Nakamura, S. DenBaars, J. Speck, and C. Weisbuch, "High-brightness polarized light-emitting diodes," Light Sci. Appl. **1**(8), e22 (2012).
14. K. McGroddy, A. David, E. Matioli, M. Iza, S. Nakamura, S. DenBaars, J. S. Speck, C. Weisbuch, and E. L. Hu, "Directional emission control and increased light extraction in GaN photonic crystal light emitting diodes," Appl. Phys. Lett. **93**(10), 103502 (2008).
15. H. Jeong, Y. H. Kim, T. H. Seo, H. S. Lee, J. S. Kim, E.-K. Suh, and M. S. Jeong, "Enhancement of light output power in GaN-based light-emitting diodes using hydrothermally grown ZnO micro-walls," Opt. Express **20**(10), 10597–10604 (2012).
16. S. J. An, J. H. Chae, G.-C. Yi, and G. H. Park, "Enhanced light output of GaN-based light-emitting diodes with ZnO nanorod arrays," Appl. Phys. Lett. **92**(12), 121108 (2008).
17. B. H. Kim and J. W. Kwon, "Metal catalyst for low-temperature growth of controlled zinc oxide nanowires on arbitrary substrates," Sci. Rep. **4**, 4379 (2014).
18. K.-K. Kim, S. Lee, H. Kim, J.-C. Park, S.-N. Lee, Y. Park, S.-J. Park, and S.-W. Kim, "Enhanced light extraction efficiency of GaN-based light-emitting diodes with ZnO nanorod arrays grown using aqueous solution," Appl. Phys. Lett. **94**(7), 071118 (2009).
19. K. S. Kim, S.-M. Kim, H. Jeong, M. S. Jeong, and G. Y. Jung, "Enhancement of light extraction through the wave-guiding effect of ZnO sub-microrods in InGaN blue light-emitting diodes," Adv. Funct. Mater. **20**(7), 1076–1082 (2010).
20. J. Zhong, H. Chen, G. Saraf, Y. Lu, C. K. Choi, J. J. Song, D. M. Mackie, and H. Shen, "Integrated ZnO nanotips on GaN light emitting diodes for enhanced emission efficiency," Appl. Phys. Lett. **90**(20), 203515 (2007).
21. H. Jeong, D. J. Park, H. S. Lee, Y. H. Ko, J. S. Yu, S.-B. Choi, D.-S. Lee, E.-K. Suh, and M. S. Jeong, "Light-extraction enhancement of a GaN-based LED covered with ZnO nanorod arrays," Nanoscale **6**(8), 4371–4378 (2014).
22. B. Liu and H. C. Zeng, "Hydrothermal synthesis of ZnO nanorods in the diameter regime of 50 nm," J. Am. Chem. Soc. **125**(15), 4430–4431 (2003).
23. Z.-P. Sun, L. Liu, L. Zhang, and D.-Z. Jia, "Rapid synthesis of ZnO nano-rods by one-step, room-temperature, solid-state reaction and their gas-sensing properties," Nanotechnology **17**(9), 2266–2270 (2006).
24. H. Jeong, S. Y. Jeong, D. J. Park, H. J. Jeong, S. Jeong, J. T. Han, H. J. Jeong, S. Yang, H. Y. Kim, K.-J. Baeg, S. J. Park, Y. H. Ahn, E.-K. Suh, G.-W. Lee, Y. H. Lee, and M. S. Jeong, "Suppressing spontaneous polarization of p-GaN by graphene oxide passivation: Augmented light output of GaN UV-LED," Sci. Rep. **5**, 7778 (2015).
25. D. Singh, A. A. Narasimulu, L. Garcia-Gancedo, Y. Q. Fu, T. Hasan, S. S. Lin, J. Geng, G. Shao, and J. K. Luo, "Vertically aligned smooth ZnO nanorod films for planar device applications," J. Mater. Chem. C Mater. Opt. Electron. Devices **1**(14), 2525–2528 (2013).
26. G. Zou, H. Luo, Y. Zhang, J. Xiong, Q. Wei, M. Zhuo, J. Zhai, H. Wang, D. Williams, N. Li, E. Bauer, X. Zhang, T. M. McCleskey, Y. Li, A. K. Burrell, and Q. X. Jia, "A chemical solution approach for superconducting and hard epitaxial NbC film," Chem. Commun. (Camb.) **46**(41), 7837–7839 (2010).
27. Y. Gong, T. Andelman, G. Neumark, S. O'Brien, and I. Kuskovsky, "Origin of defect-related green emission from ZnO nanoparticles: effect of surface modification," Nanoscale Res. Lett. **2**(6), 297–302 (2007).
28. G. Pezzotti and W. Zhu, "Resolving stress tensor components in space from polarized Raman spectra: polycrystalline alumina," Phys. Chem. Chem. Phys. **17**(4), 2608–2627 (2015).
29. R. Zhang, P.-G. Yin, N. Wang, and L. Guo, "Photoluminescence and Raman scattering of ZnO nanorods," Solid State Sci. **11**(4), 865–869 (2009).
30. Y. Ono, Y. Kimura, Y. Ohta, and N. Nishida, "Antireflection effect in ultrahigh spatial-frequency holographic relief gratings," Appl. Opt. **26**(6), 1142–1146 (1987).
31. T. Koschny, M. Kafesaki, E. N. Economou, and C. M. Soukoulis, "Effective medium theory of left-handed materials," Phys. Rev. Lett. **93**(10), 107402 (2004).

1. Introduction

GaN-based light-emitting diodes (LEDs) are currently driving a revolution in the field of solid-state lighting, signaling, and large displays because they are expected to replace traditional illumination sources, such as light bulbs, incandescent electric lamps, and

#246197 Received 16 Jul 2015; revised 22 Aug 2015; accepted 24 Aug 2015; published 25 Aug 2015

fluorescent lamps [1–4]. This is because of their significantly lower energy consumption, longer lifetime, and higher light emission efficiency compared to those of traditional light sources [5–7]. However, the light-extraction efficiency (LEE) of GaN-based LEDs is still low by means of the total internal reflection (TIR) of photons generated in LEDs. This TIR is caused by the large difference between the refractive indices of the LED and air [8]. To improve the LEE, many research groups have suggested various solutions, such as graded-refractive-index indium tin oxide (ITO) [9,10], intentionally roughening the LED surface [11,12], photonic crystal slabs [13,14], and ZnO micro-/nano-structures grown on the LEDs with a hydrothermal method [15,16]. In particular, the formation of ZnO micro-/nano-structures on the surface of GaN-based LEDs with a hydrothermal method is the most acceptable technique for increasing the LEE of LEDs because it is a simple process performed on the completed LED chips [17]. Moreover, the hydrothermal method of growing ZnO micro-/nano-structures is the most promising for practical applications because of the simplicity, short growth time, low cost, and low temperature of the process, which does not change the electrical properties of the LEDs [18,19]. For these reasons, several research groups have investigated the hydrothermal growth of ZnO nanorods (NRs) on the surface of GaN-based LEDs to enhance their light output power. To explain the increased LEE of such LEDs, Zhong *et al*. [20] suggested the ZnO NRs create a gradual variation in the effective refractive index. In addition, Jeong *et al*. [21] reported experimental and theoretical results that showed a reduction in the Fresnel reflections occurring at the interface between the LED and air. In addition, LEE of LED grown on patterned sapphire substrate is also remarkably influenced by ZnO NRs [21]. However, optimization of ZnO NRs for improving LEE of LEDs by controlling the length and the effective refractive index of ZnO NRs has not been reported previously. In this study, we investigated optimal length of ZnO NRs which were grown with a hydrothermal method for improving LEE of blue InGaN LEDs. For comparison purposes, different lengths of ZnO NRs were grown on the blue GaN-based LEDs: short ZnO NRs, which have been tested by several research groups [22,23], and long ZnO NRs. Furthermore, simulations based on three-dimensional (3D) finite-difference time-domain (FDTD) analysis were performed to support our experimental results. Scanning electron microscopy (SEM) was used to observe the morphology of the ZnO NRs grown on the blue GaN-based LEDs. The crystal structure of the ZnO NRs grown was determined with X-ray diffraction (XRD). Macro-photoluminescence (macro-PL) and micro-Raman spectroscopies were employed to measure the optical and structural properties of the ZnO NRs. The device performance was determined from the light output power as a function of the injection current and current versus voltage curves.

2. Experiment

To induce the self-assembly of the ZnO NRs, an accurate amount of zinc acetate dihydrate [$Zn(O_2CCH_3)_2(H_2O)_2$] was dissolved in deionized water to produce a 0.05 M solution at room temperature. Ammonium hydroxide (NH_4OH) was employed to form an alkaline reaction environment (pH 9) in the solution. A 0.005 M solution of zinc acetate dihydrate dissolved in ethanol was spread on the surface of the prepared LED chips and heated at 300 °C for 20 min. All hydrothermal processes were performed for 60 min at 150 °C in an autoclave. The pressure and heating rate in the autoclave were 4 atm and 3 °C/s, respectively. The growth conditions for the ZnO NRs were identical for all of the samples. Laser holographic lithography was used to fabricate periodic patterns on the surface of the LEDs. A positive photoresist (PR) was mixed with a thinner and spin-coated onto the ZnO seed layer, which was followed by a soft-baking process at 110 °C for 1 min. To illuminate areas of the PR selectively, a He-Cd laser (λ = 325 nm) was employed. Half of the laser beam directly irradiated the photoresist, and the other half was projected onto the photoresist after being reflected from a Lloyd mirror. These two beams created an interference pattern on the PR, which resulted in a sinusoidal exposure. To achieve a square lattice pattern, the sample was

#246197 Received 16 Jul 2015; revised 22 Aug 2015; accepted 24 Aug 2015; published 25 Aug 2015

rotated by 90° and exposed to the laser again. The exposed area of the PR was removed with a developer. After the exposed PR was removed, only a periodic pattern of holes remained on the surface of the LED. Field emission scanning electron microscopy (FE-SEM, S-4700, Hitachi) was used to observe the surface morphology and cross sections of the samples. The crystal structure of the ZnO NRs was clarified with XRD. Macro-PL spectroscopy with a He-Cd laser (λ = 325 nm) was performed to investigate the optical properties of the ZnO NRs. To verify the crystal structure of the ZnO NRs, micro-Raman scattering measurements were performed with a He-Ne laser (λ = 633 nm). The light output power of the LEDs was measured from the top of the LEDs with a Si photodiode connected to an optical power meter. The electrical properties of the devices were measured with a conventional probe station system equipped with a Keithley SourceMeter 2400. The 3-dimensional (3D) finite-difference time-domain (FDTD) simulations were used to investigate if the theoretical calculations corresponded with the experimental results.

3. Results and discussion

The blue InGaN LED epitaxial structures were grown by metal-organic chemical vapor deposition. During the crystal growth process, H_2 was used as the carrier gas, except when N_2 was used to fabricate the InGaN/GaN multiple quantum wells (MQWs). The LED chips were grown on a *c*-plane sapphire substrate, with the layers sequentially deposited in the following order: a 2-μm-thick undoped GaN layer on a 20-nm-thick GaN nucleation layer, a 2-μm-thick n-type GaN layer, 7 pairs of InGaN/GaN MQWs acting as the active region, a p-type AlGaN carrier-blocking layer, a 150-nm-thick p-GaN layer, and Mg-doped, graded, p^{++}GaN layers. To activate the hole carriers of the p-GaN layer, the epitaxial LED structure was annealed with rapid thermal annealing at 940 °C for 40 s. For the metallization of the n-GaN layer, the epitaxial LED layers were partially etched down to the n-type GaN layer with inductively coupled plasma etching using a $Cl_2/BCl_3/Ar$ plasma. Using conventional photolithography and metal deposition techniques, we obtained LED arrays with ITO as the current spreading layer and Cr/Au as the p-n-type electrode. Figure 1(a) shows the electroluminescence (EL) spectrum of a fully fabricated blue InGaN LED, which was measured at an operating current of 20 mA. The peak wavelength of the EL spectrum is at 455 nm and the inset shows a 3D schematic of the final structure of the LED. Figure 1(b) shows a magnified 3D schematic of the fabricated blue InGaN LEDs with simple descriptions of each layer. It should be noted that we have used a commercially optimized epitaxial LED structure with a p-AlGaN carrier-blocking layer and Mg-doped, graded, p^{++}GaN layers to produce LEDs with a high internal quantum efficiency [24]. In general, the length of the ZnO NRs is mainly determined by the growth time and concentration of the seed solution. Using the growth conditions described in the Materials and Methods section, the ZnO NRs obtained are shorter than 500 nm.

#246197 Received 16 Jul 2015; revised 22 Aug 2015; accepted 24 Aug 2015; published 25 Aug 2015

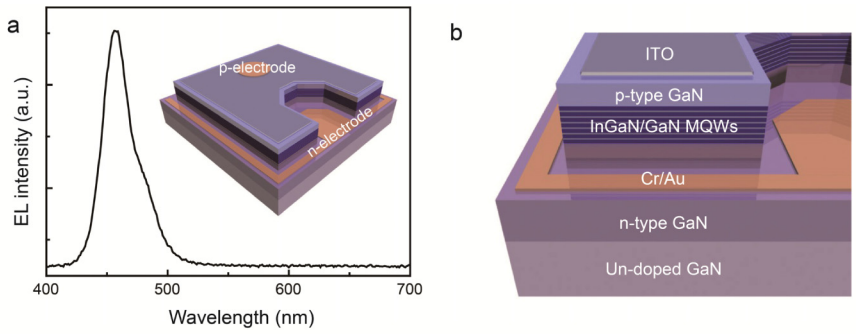

Fig. 1. Fully fabricated blue InGaN light-emitting diode (LED). (a) Electroluminescence spectrum of the fabricated blue InGaN LED. The peak wavelength of the LED is at 455 nm. The inset shows a 3-dimensional (3D) schematic of the final structure of the LED with Cr/Au electrodes as the n-p contacts. (b) A magnified 3D schematic of the LED structure, with the individual layers labeled.

If the growth time is increased to 10 h to obtain 5-μm-long ZnO NRs, the manufacturing yield is significantly reduced. Moreover, if the concentration of zinc acetate dihydrate in the deionized water is increased to achieve longer ZnO NRs, the ZnO NRs could merge with each other. To avoid such problems, we applied laser-based holographic lithography (LHL) to the ZnO seed layer to produce remarkably long ZnO NRs while using the same conditions described in the Materials and Methods section. For comparison purposes, ZnO NRs with two different lengths were fabricated on the blue InGaN LEDs. The first length was achieved by growing the ZnO NRs directly on the surface of the LEDs without any additional treatments. The second length was achieved by growing the ZnO NRs through the periodically patterned photoresist formed with LHL on the surface of the LEDs. Figure 2(a) shows a schematic of how the LED chip was prepared to obtain the longer ZnO NRs. The 0.005 M solution of zinc acetate dihydrate in high-purity ethanol was deposited on the surface of the LEDs as a seed layer for the ZnO NRs. For the LHL process, a positive PR was spin-coated on top of the seed layer. A double exposure of the LHL process was then conducted on the PR layer to form a periodic pattern of holes. After developing the PR, we obtained a layer with a periodic pattern of holes that exposed the seed layer, which is depicted in Fig. 2(b). The hydrothermal growth of the ZnO NRs was then initiated on the LHL-prepared LED. The periodically exposed seed layer was where the nucleation and growth of the ZnO NRs occurred, as illustrated in Fig. 2(c). After the hydrothermal growth of the ZnO NRs, the sample was dipped in acetone to remove the remaining PR. Finally, the periodically arranged ZnO NRs were obtained, as shown in Fig. 2(d). Figure 2(e) shows a plane-view SEM image of the periodic pattern of holes formed in the PR by the LHL process. The periodicity and diameter of the holes are approximately 400 nm and 300 nm, respectively. Figure 2(f) shows a cross-sectional SEM image of the ZnO NRs that have grown through the periodically patterned PR (the PR was removed before taking this image). The length of the ZnO NRs grown on the LHL-treated LED chips is approximately 5 μm. Figure 2(g) is a magnified cross-sectional SEM image of the bottom of the ZnO NRs that shows the truncated cone shape of the NRs. This shape indicates that the initial growth of the ZnO NRs occurred within the holes of the periodically patterned layer. The reason why the size of the circular pattern present in Fig. 2(g) is larger than the holes shown in Fig. 2(e) is the undercutting of the PR, which typically occurs during the developing process. The cross-sectional SEM image shown in Fig. 2(h) also presents the bottom of the ZnO NRs.

#246197 Received 16 Jul 2015; revised 22 Aug 2015; accepted 24 Aug 2015; published 25 Aug 2015

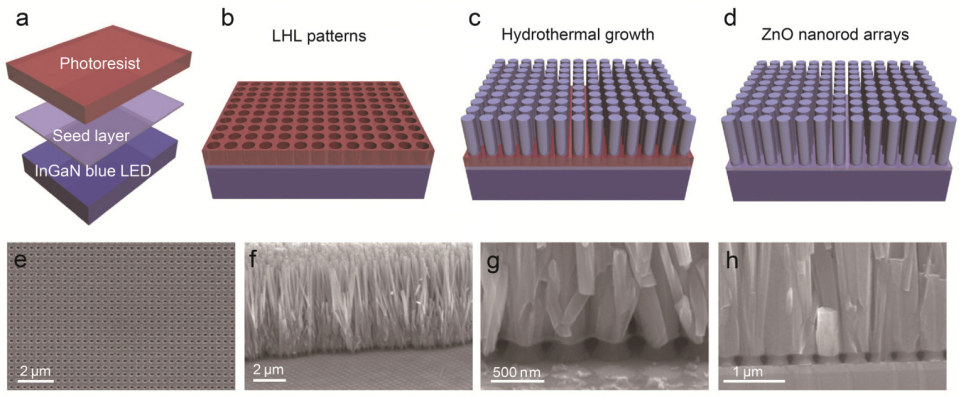

Fig. 2. Fabrication of ZnO nanorods (NRs) on the blue InGaN LEDs. 3D schematics of the: (a) blue InGaN LED, ZnO seed layer, and photoresist (PR) layer used for the laser holographic lithography (LHL) process, (b) periodic pattern of holes in the PR, and the ZnO NRs grown through the holes of the LHL-patterned PR layer (c) before and (d) after the PR layer is removed (e) Plane-view scanning electron microscopy (SEM) image of the LHL-patterned PR layer. (f) Cross-sectional SEM image of the ZnO NRs grown on the surface of the LED through the LHL-patterned PR layer. (g) A magnified SEM image of the bottom of the ZnO NRs. (h) Cross-sectional SEM image of the ZnO NRs formed on the surface of the LED.

The periodic vacancies revealed in this SEM image are further evidence that the ZnO NRs are selectively grown in the holes of the patterned PR. Since the growth conditions were identical for both the ZnO NRs with and without the periodically patterned PR layer, the longer length of the ZnO NRs with the patterned PR is caused by the selective-area growth.

Since the optical properties of the ZnO NRs could be influenced by the LEDs, *c*-plane sapphire substrates were employed instead of the GaN-based LEDs for the structural and optical characterization of the ZnO NRs. Cross-sectional SEM images of the ZnO NRs grown on the surface of the LEDs with and without the LHL-patterned PR layer are presented in Figs. 3(a) and 3(b), respectively. The final lengths of the ZnO NRs grown on the LEDs with and without the LHL-patterned PR layer are approximately 5 μm and 300 nm, and their growth rates are 1.533 nm/s and 0.083 nm/s, respectively. Consequently, the ZnO NRs grown with the LHL-patterned PR layer are more than 16-times longer than those directly grown on the sapphire substrate without the LHL-patterned PR layer due to exceptionally higher growth rate induced by selective area growth of *c*-plane ZnO.

#246197 Received 16 Jul 2015; revised 22 Aug 2015; accepted 24 Aug 2015; published 25 Aug 2015

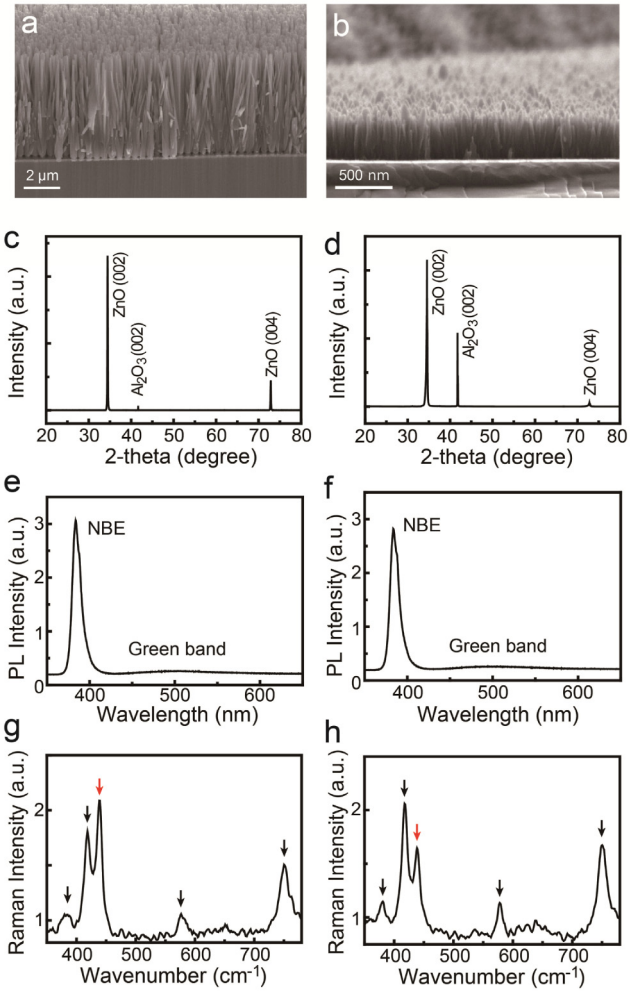

Fig. 3. Optical and structural properties of the ZnO NRs. Cross-sectional SEM images of the ZnO NRs grown on the surface of the LEDs (a) with and (b) without the LHL-patterned PR layer. X-ray diffraction (XRD) patterns of the ZnO NRs grown on *c*-plane sapphire substrates (c) with and (d) without the LHL-patterned PR layer. PL spectra of the ZnO NRs (e) grown with and (f) without the LHL-patterned PR layer. Raman spectra of the ZnO NRs grown on a *c*-plane sapphire substrates (g) with and (h) without the LHL-patterned PR layer.

To determine the crystal structures of both types of ZnO NRs, XRD measurements were performed. The two-theta curves scanned over 20° to 80° for the ZnO NRs grown with and without the LHL-patterned PR layer are shown in Figs. 3(c) and 3(d), respectively. As can be seen, there are strong peaks at 34.2° and 72.5° in both XRD patterns, which correspond to the (002) and (004) planes of ZnO, respectively [25]. The peak at 41.3° is caused by the *c*-plane sapphire substrate [26]. The other characteristic peaks of ZnO are not present in the XRD patterns of the ZnO NRs. This implies that the ZnO NRs grown with and without the LHL-patterned layer are homogeneously formed along the *c*-axis. It should be noted that the intensity of the sapphire (002) peak varies with the length of the ZnO NRs because the X-rays must pass through the NRs to reach the sapphire substrate. The optical properties of both types of ZnO NRs were measured with macro-PL spectroscopy. The PL spectra of the ZnO NRs grown with and without the LHL-patterned PR layer are shown in Figs. 3(e) and 3(f),

#246197 Received 16 Jul 2015; revised 22 Aug 2015; accepted 24 Aug 2015; published 25 Aug 2015

respectively. Both spectra exhibit a strong peak at 380 nm with a narrow bandwidth, which is caused by the near-band-edge (NBE) transitions of excitons, and a weak peak at 500 nm with a broad bandwidth, which is related to crystal defects in the NRs [27]. The strong NBE peak with a negligible green emission band indicates that the ZnO NRs have high crystallinity and good optical properties. To verify the crystal structure of the ZnO NRs, micro-Raman spectroscopy was performed in the back scattering geometry. Figures 3(g) and 3(h) show the Raman spectra of the ZnO NRs grown with and without the LHL-patterned PR layer on *c*-plane sapphire substrates. The peaks marked with black arrows at 379, 418, 578, and 751 cm^{-1} in both Raman spectra are the Raman modes of the *c*-plane sapphire substrates [28]. The peak at 439 cm^{-1} in the Raman spectra, indicated with red arrows, is the E_2^{high} optical phonon mode of ZnO with a hexagonal wurtzite crystal structure [29]. The relatively high intensity of the E_2^{high} optical phonon in the Raman spectrum of the ZnO NRs grown with the LHL-patterned PR layer is attributed to the larger volume of the ZnO NRs. Through the structural and optical characterization of the ZnO NRs, we can conclude that the ZnO NRs grown with and without the LHL-patterned PR layer have almost identical structural and optical properties.

The device performance of the blue InGaN LEDs with and without the ZnO NRs was verified by measuring the light output power versus the injection current (L-I) and current-voltage (I-V) curves. The chip size of the LED used in this study is 300 × 300 μm. L-I curves of the conventional blue InGaN LED (black line), and blue InGaN LEDs with the 300-nm- (blue line) and 5-μm-long (red line) ZnO NRs are shown in Fig. 4(a). The light output power of the LEDs with the 300-nm- and 5-μm-long ZnO NRs are approximately 14.6% and 40.7% greater, respectively, than that of the LED without the ZnO NRs at an operating current of 20 mA.

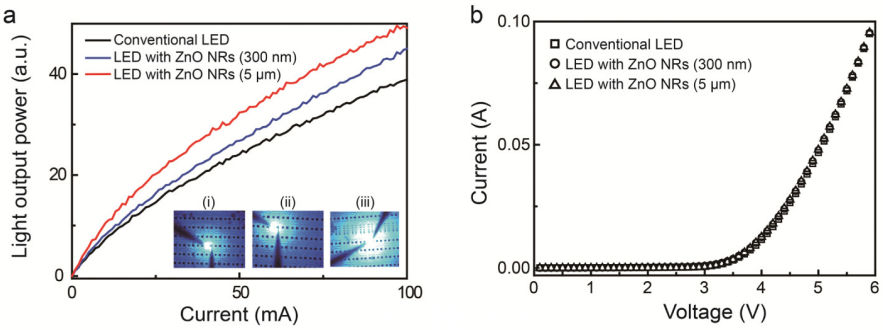

Fig. 4. Device performance. (a) Light output power versus current (L-I) curves of the conventional LED and LEDs with the 300-nm- and 5-μm-long ZnO NRs. The insets show optical microscope images of the (i) conventional LED, (ii) LED with 300-nm-long ZnO NRs, and (iii) LED with 5-μm-long ZnO NRs operating at 5 mA. (b) Current versus voltage (I-V) curves of the conventional LED and LEDs with the 300-nm- and 5-μm-long ZnO NRs.

The insets (i), (ii), and (iii) are optical microscope images of the conventional LED, and LEDs with the 300-nm- and 5-μm-long ZnO NRs at an injection current of 5 mA, respectively. The LED with the 5-μm-long ZnO NRs has significantly higher light output power compared to the other LEDs. Since the structural and optical properties of the ZnO NRs are almost identical for both lengths of the ZnO NRs, this difference in the enhancement of the light output power is caused by the different lengths of the ZnO NRs grown on the surface of the LEDs. Figure 4(b) shows the I-V curves of the conventional LED (squares) and LEDs with the 300-nm- (circles) and 5-μm-long (triangles) ZnO NRs. As can be seen, the I-V curves of the samples are almost identical, which means that there are no differences in the electrical properties of the LEDs. This is further evidence that the electrical properties of the

#246197 Received 16 Jul 2015; revised 22 Aug 2015; accepted 24 Aug 2015; published 25 Aug 2015

devices are not affected by the ZnO NRs grown on the surface of the LEDs, regardless of the different lengths of the NRs. Therefore, these experimental results indicate that the LEE of LEDs with ZnO NRs is strongly influenced by the length of the ZnO NRs. To verify the effects of the length of the ZnO NRs on the LEE of the LEDs, we simulated light propagation through the ZnO NRs on the LEDs with a 3D FDTD method. First, we defined the refractive index of each layer of the fully fabricated, blue, InGaN LED at a wavelength of 450 nm, which corresponds to the emission wavelength of the LED. The refractive indices of the p-type and n-type GaN were fixed at 2.5, whereas the refractive index of the MQW layer was set to 2.6. The refractive index of the ZnO NR layer was set to 1.8, which is the effective refractive index calculated with effective-medium theory [30,31]. At the top of the ZnO NR layer, the effective refractive index varies from approximately 1.8 to 1.0 because of the inhomogeneous volume fraction of the ZnO NRs. The variation of refractive index along the vertical structure of the LEDs with and without the ZnO NRs is depicted in Fig. 5(a).

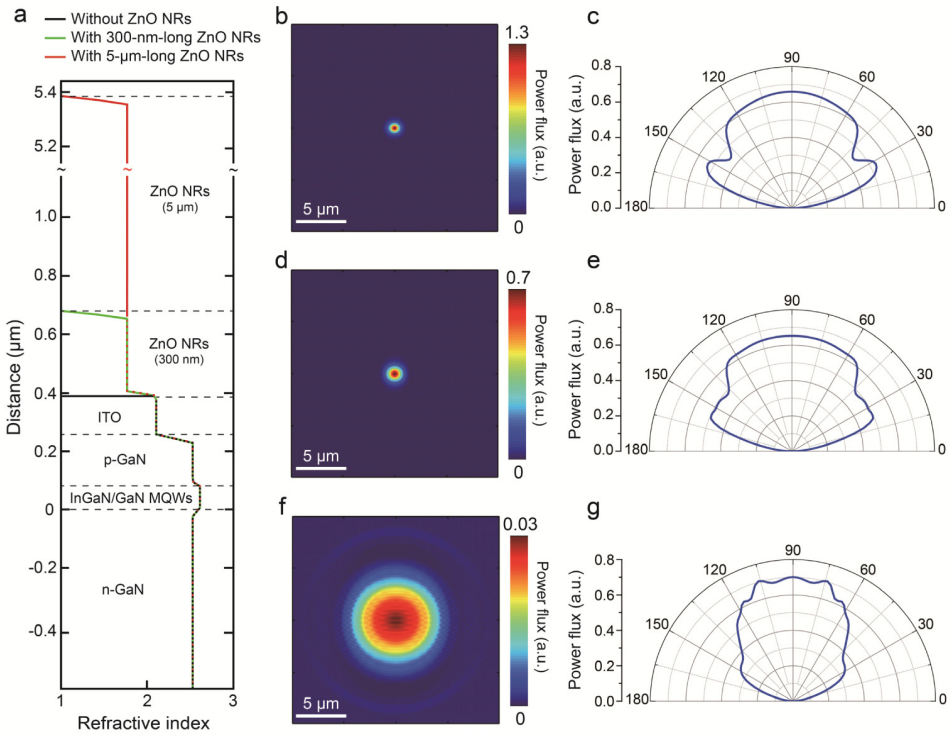

Fig. 5. 3D finite-difference time-domain (FDTD) analysis. (a) The variation of refractive index along the vertical structure of the LEDs with and without the ZnO NRs. The FDTD images calculated for the optical power of the (b) conventional LED, (d) LED with 300-nm-long ZnO NRs, and (f) LED with 5-μm-long ZnO NRs. Calculated far-field radiation patterns of the (c) conventional LED, (e) LED with 300-nm-long ZnO NRs, and (g) LED with 5-μm-long ZnO NRs.

The black line indicates the refractive indices of the conventional LED structure without the ZnO NRs. The green and red lines show the refractive indices of the LEDs with the 300-nm- and 5-μm-long ZnO NRs, respectively. As shown in Fig. 5(a), the refractive index of the GaN-based LEDs with the ZnO NRs gradually decreases from the active layer of the LED to air. For the 3D FDTD simulations, we used perfectly matched layers (PML) as the boundary conditions for all boundaries. In addition, a non-uniform mesh was used during the simulations. The grid size was 30 nm in the bulk region and 3 nm near the interfaces of the materials along the x-, y-, and z-axes. We placed a monitor at (x, y_{top}, z) to calculate the

#246197 Received 16 Jul 2015; revised 22 Aug 2015; accepted 24 Aug 2015; published 25 Aug 2015

power flow (*i.e.*, the y-component of the Poynting vector) through the surface of the monitor. In addition, we placed four more side monitors above the surface of the ITO to monitor the radiated light in 3D. The sum of the optical power flowing through these four monitors plus the top monitor gives the total optical power radiated by the LED. Finally, four more side monitors were placed under the surface of the ITO layer to measure the optical power loss, *i.e.*, the light that does not escape the LED. The FDTD images calculated for the optical power of the conventional LED without the ZnO NRs is shown in Fig. 5(b). The light source is a single electric dipole oriented along the x-axis. The FDTD images calculated for the LEDs with the 300-nm- and 5-μm-long ZnO NRs are shown in Figs. 5(d) and 5(f), respectively. As can be seen, the size of the circular light detected increases as the length of the ZnO NRs increase, but the maximum optical power is the achieved by the LED without the ZnO NRs. However, it should be noted that the integrated optical power of the LED with the 5-μm-long ZnO NRs is much higher than that of the LEDs without and with the300-nm-long ZnO NRs (see Table 1). The far-field radiation patterns of the light radiated from the surface of the LEDs was also calculated with 3D FDTD simulations for a dipole oriented along the x-axis. The far-field radiation pattern of the conventional LED without the ZnO NRs is shown in Fig. 5(c). As can be seen, the lateral light intensity is nearly equal to the vertical light intensity because of considerably high Fresnel reflection occurred at the interfaces between GaN, ITO, and air. Figures 5(e) and 5(g) show the far-field radiation patterns of the LEDs with the 300-nm- and 5-μm-long ZnO NRs, respectively. The lateral light intensity of the LED with the 300-nm-long ZnO NRs is lower than that of the conventional LED. This is attributed to the decreased Fresnel reflections at the interface between the ITO and ZnO NRs, which is caused by the decreased difference between the refractive indices. However, the vertical light intensity is almost equivalent to that of the conventional LED. In the far-field radiation pattern of the LED with the 5-μm-long ZnO NRs, the lateral light intensity is significantly reduced and the vertical light intensity is enhanced compared to that of the LEDs without and with the 300-nm-long ZnO NRs. This indicates that more photons were vertically guided to the surface by the longer ZnO NR layer than that guided by the shorter ZnO NRs. This suggests that the number of waveguide modes with a specific light propagation direction is closely related to the thickness of the optical waveguide layer. To calculate the LEE enhancement factor as a function of the length of the ZnO NRs, the LEE of the LEDs was defined as the ratio of the optical power radiated above the LED within the desired range of angles to the optical power emitted by the active layer. The LEE is calculated with the following equation: $LEE = P_{rad}/(P_{rad} + P_{loss})$ where P_{rad} and P_{loss} are the radiated optical power and loss, respectively. Furthermore, to take into account the randomly polarized nature of the LEDs, we separately simulated the optical power emitted by a single electric dipole source oriented in three orthogonal directions and then summed the results incoherently. The dipole sources, with the emission wavelength fixed at 450 nm, were placed at the center of the xz-plane in the middle of the active layer. The LEE of the LEDs was calculated by taking the ratio of the optical power radiated above the ITO surface to the optical power emitted by the dipole. The LEE enhancement factor is defined as the ratio of the LEE of an LED with a ZnO NR layer to the LEE of a bare LED. Table 1 shows the results of the 3D FDTD calculations for an x-oriented dipole.

#246197 Received 16 Jul 2015; revised 22 Aug 2015; accepted 24 Aug 2015; published 25 Aug 2015

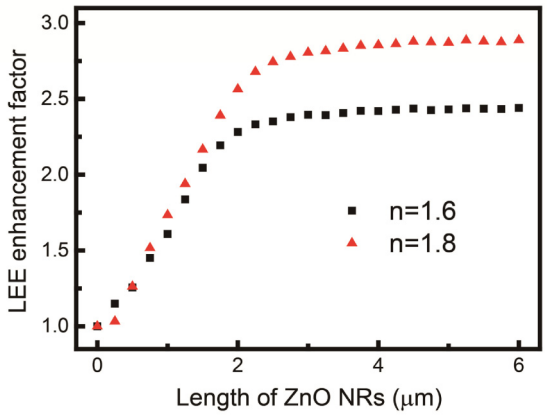

Fig. 6. Light-extraction efficiency (LEE) enhancement factor of the blue InGaN LEDs as a function of the thickness of the optical waveguide layer on the LED.

The P_{rad} increases as the length of the ZnO NRs increases because of the increasing number of waveguide modes. The trends shown by the P_{rad} and LEE of the samples are in accordance with the experimental results [Fig. 4(a)]. Moreover, similar values of P_{loss_LED} are obtained for the LEDs with the 300-nm- and 5-μm-long ZnO NRs, and they are much smaller than that of the conventional LED, which supports the hypothesis of reduced Fresnel reflections at the interface between the ITO and air when the ZnO NRs are applied to the surface of the LEDs. The calculated results for the y- and z-oriented dipoles are presented in Table 1. The parameters for the y- and z-oriented dipoles follow the trends of x-oriented dipole parameters except P_{loss_LED}. Based on the values calculated for these factors, we obtained the average LEE and LEE enhancement factor, as shown in Table 1. The difference between the theoretical and experimental enhancement values is attributed to the non-uniform length of the ZnO NRs and losses associated with the experimental photodetector setup. However, the trend of the theoretically calculated LEE enhancements is remarkably close to the experimentally measured light output power. Figure 6 shows the LEE enhancement factor of the x-oriented dipole as a function of the length of the ZnO NRs on the surface of the LEDs, which was calculated with FDTD. To account for the slightly different volume fraction of the LHL-patterned ZnO NRs compared to the conventional ZnO NRs, we used effective refractive indices of 1.8 and 1.6, respectively. The black squares and red triangles indicate the effective refractive indices of 1.6 and 1.8, respectively. As the length of the ZnO NRs increases from 0 to 2 μm, the LEE enhancement factor increases linearly for both effective refractive indices, but the LEE enhancement factor for an effective refractive index of 1.6 becomes saturated above 2 μm. For the effective refractive index of 1.8, the saturation point is approximately 2.5 μm. These results support the hypothesis that the number of waveguide modes and the effective refractive index significantly affect the LEE enhancement factor. Moreover, these results signify that the number of waveguide modes that pass through the ZnO NRs on the surface of the LEDs becomes saturated depending on the length of the ZnO NRs. According to these calculations, the difference between the enhancement values obtained from the experiments and theoretical calculations can be explained by the non-uniform effective refractive index along the ZnO NR layer because of the partially inhomogeneous ZnO NRs. Nevertheless, the theoretical and experimental results indicate that the light output power of blue InGaN LEDs is highly sensitive to the length of the ZnO NRs grown on the surface of the LEDs.

#246197 Received 16 Jul 2015; revised 22 Aug 2015; accepted 24 Aug 2015; published 25 Aug 2015

Table 1. FDTD-calculated parameters for a dipole oriented along the x-, y-, and z-axes (λ = 450 nm).

	H_{ZnO} = 0 (x-dipole)	H_{ZnO} = 300 nm (x-dipole)	H_{ZnO} = 5 μm (x-dipole)
P_{rad} (P_{top} + P)	0.037	0.0492	0.158
$P_{loss\ LED}$	0.0856	0.089	0.0886
$P_{loss\ sub}$	0.157	0.157	0.155
LEE_x	13.7%	16.6%	39.4%
$LEE_{enhancement,x}$	1	1.2	2.9
	H_{ZnO} = 0 (y-dipole)	H_{ZnO} = 300 nm (y-dipole)	H_{ZnO} = 5 μm (y-dipole)
P_{rad} (P_{top} + P)	0.035	0.0049	0.05
$P_{loss\ LED}$	0.0946	0.1096	0.1078
P_{loss_sub}	0.391	0.389	0.389
LEE_y	0.7%	0.9%	0.9%
$LEE_{enhancement,y}$	1	1.3	1.3
	H_{ZnO} = 0 (z-dipole)	H_{ZnO} = 300 nm (z-dipole)	H_{ZnO} = 5 μm (z-dipole)
P_{rad} (P_{top} + P)	0.038	0.0497	0.156
$P_{loss\ LED}$	0.0852	0.0899	0.0881
$P_{loss\ sub}$	0.1577	0.1577	0.1555
LEE_z	13.7%	16.6%	39.4%
$LEE_{enhancement,z}$	1	1.2	2.9
	H_{ZnO} = 0 (Average)	H_{ZnO} = 300 nm (Average)	H_{ZnO} = 5 μm (Average)
LEE_{avg}	9.3%	11.4%	26.6%
$LEE_{enhancement,avg}$	1	1.2	2.4

4. Conclusion

We have experimentally demonstrated and theoretically analyzed the NR-length-dependent enhanced light output power and LEE of blue InGaN LEDs with ZnO NRs. The experimental results indicated that the hydrothermally grown ZnO NRs were highly crystalline and vertically well aligned with respect to the substrate. With conventional L-I and I-V measurements, we found that the light output power of the LEDs with the 300-nm- and 5-μm-long ZnO NRs was approximately 14.6% and 40.7% greater, respectively, than that of the LED without the ZnO NRs at an operating current of 20 mA. However, the electrical properties of the devices were not significantly affected by the ZnO NRs. The effects of the length of the ZnO NRs on the LEE of the LEDs were verified with 3D FDTD analysis. The FDTD-calculated images of the optical power and far-field radiation patterns indicated that more photons were guided to the surface of the LED by the longer ZnO NR layer than by the shorter ZnO NR layer, which suggests the number of waveguide modes depends on the thickness of the optical waveguide layer. The theoretical LEE values calculated for a single dipole source oriented in three orthogonal directions supported the experimental results and

#246197 Received 16 Jul 2015; revised 22 Aug 2015; accepted 24 Aug 2015; published 25 Aug 2015

showed that the length of the ZnO NR layer on the surface of the LEDs significantly affects the LEE enhancement of the LED. Finally, we found optimal length of ZnO NR to enhance the light-extraction efficiency of InGaN LEDs, which is attributed to increased number of waveguide modes. We believe that our verification of the length-dependent light-extraction mechanism of the ZnO NRs on the surface of the blue InGaN LEDs could ultimately lead to high-efficiency LEDs for general lighting applications.

Acknowledgment

This work was partially by the FUI MULTISS project (F1305008 M) and supported by IBS-R011-D1 of Korea.

#246197 Received 16 Jul 2015; revised 22 Aug 2015; accepted 24 Aug 2015; published 25 Aug 2015